Radiation Physics and Chemistry 117 (2015) 198–202

Contents lists available at ScienceDirect

Radiation Physics and Chemistry

journal homepage: www.elsevier.com/locate/radphyschem

Optimal configuration for detection of gold nanoparticles in tumors using Kβ X-ray fluorescence line

R.G. Figueroa [a,*], M. Santibañez [a], F. Malano [b], M. Valente [b]

[a] Departamento de Ciencias Físicas, University of La Frontera, Avenida Francisco Salazar, 01145 Temuco, Chile
[b] Institute of Physics E. Gaviola–CONICET LIIFAMIRx – University of Córdoba Ciudad Universitaria, 5000 Cordoba, Argentina

HIGHLIGHTS

- Optimal detection of gold nanoparticles in tumors.
- Monte Carlo simulation of *in vivo* XRF spectroscopy in biomedical application.
- Improve in the detection limit and uncertainty of Kβ X-ray fluorescence line.

ARTICLE INFO

Article history:
Received 19 January 2015
Received in revised form
24 August 2015
Accepted 25 August 2015
Available online 28 August 2015

Keywords:
Gold nanoparticles
XMI-MSIM
In vivo EDXRF spectrometry
Monte Carlo simulation

ABSTRACT

This study examines the increase in the capacity to detect gold nanoparticles in tumor tissue using X-rays from orthovoltage sources. The analyzed methodology considered aspects of geometry and composition in accordance with those required in real clinical treatment applications. The results show that a geometrical backscatter configuration, an incident spectral energy synthesized to optimize statistical parameters and adequate background subtraction allow for a significant increase in the signal to noise ratio (SNR) of the secondary Kβ lines. This increase is greater than those currently reported for traditional Kα lines. Furthermore, these conditions also produce an increase in detection sensitivity, less uncertainty in results and shorter exposure times. The proposed methodology was evaluated using XMI-MSIM software for the Monte Carlo simulation fluorescent response of each element. The simulation used tumors of 1–3 cm^3, at a depth of 1–5 cm with a 0.1–1% gold nanoparticle concentration. The measurement time and the skin entrance dose by the methodology were considered for allows future quantitative surface scanning implementation.

1. Introduction

Gold nanoparticles (GNPs) have been widely used in recent years due to their applications as tumor markers (Hainfeld et al., 2006; Cheong et al., 2010), therapeutic agent activation enhancers (Wu et al., 2013; Patra et al., 2010; Jain et al., 2012), and enhancers of the dose deposited by orthovoltage beam radiotherapy (Jain et al., 2012; Roeske et al., 2007). The above has motivated research into a way in which to combine simultaneous identification and treatment of tumor tissue in one procedure. The main problem involved in detecting tumors marked with GNPs by X-Ray Fluorescence is the low SNR owing to the depth required in clinical cases and the dispersion caused by the tissue surrounding the tumor (Wu et al., 2013). An increase in GNP detection capability in a short time period would allow for superficial scans of the tumor area by dispositives of XRF imaging system studied for the detection of another element of interest (Figueroa et al., 2014), and the use of an orthovoltage beam would permit a focused dose to be administered as treatment.

An optimal qualitative and quantitative analysis of gold's fluorescence peaks requires that the SNR be increased as much as possible in order to identify the fluorescence peaks to be used in the calibration curves. The statistical figure of merit, however, will be determined by the detection limit and uncertainty criteria. These criteria will better estimate the ranges wherein a closer-to-optimal result would be provided in an increase in the count number along with a background increase.

The incident energy activation must be adjusted based on Bremsstrahlung produced by the X-Ray tubes. This is done by adjusting attenuation filters for lowest energies and tuning the spectrum's average energy, regulating the maximum electric potential difference applied (photons' maximum possible energy).

* Corresponding author.
E-mail address: rodolfo.figueroa@ufrontera.cl (R.G. Figueroa).

http://dx.doi.org/10.1016/j.radphyschem.2015.08.017
0969-806X/

The result of these configurations will be a spectrum made up of a non-symmetrical peak centered on a maximum that may be tuned.

As the incident signal obtained in the process is not a pure monochromatic beam, the central energy of the spectrum that maximizes fluorescent production will not necessarily be near the absorption edge. If the maximum spectrum energy produced is tuned to higher values, more photons able to produce a fluorescent emission will be generated. However, this also causes a shift in the Compton peak and, therefore, an increase of the background. Evaluating as change the detection limit and uncertainty in function of the incident energy, and weighing these two factors will determine which is the optimal incident spectrum for the established geometry.

In X-Ray Fluorescence (XRF) spectroscopy, the measured spectrum must be separated into the individual elemental fluorescence lines, later, a net-area associated to each line should be evaluated, in order to determine the signal′s intensity of each element and of the background level. For this, sophisticated procedures based on linear and no-linear fitting routines are commonly used when the spectrum are overlapped, where each the signal and background are modeled specially are modeled by appropriate analytical and experimental curves (Moya-Riffo et al., 2013; Santibáñez et al., 2013). Traditionally used for identification and quantification the primary Kα fluorescence lines. This is because they have a fluorescent production section that is much higher than secondary Kβ lines. However, it is more suitable to identify secondary peaks in experimental configurations in which a strong background or overlap with other peaks is present. In gold detection, its primary line strongly overlaps with the Compton peak generated by the incident beam. This translates into a lower SNR and in worse detection limits and higher uncertainty, especially when the element is at low concentrations. The low concentration of gold would require a greater concentration of these nanoparticles in tumor tissue when employed in clinical applications.

There are reports on methodologies that optimize the identification of gold's Kα fluorescence signals in applications of this type. However, the dimensions and conditions in which they have been evaluated differ greatly from the real geometries in which its implementation requires it be performed (Wu et al., 2013). Great uncertainty at low concentration (concentration below 1%) has also been reported. In the present study, optimization of gold nanoparticles inside the tumor tissue was sought by detecting secondary Kβ fluorescence lines and real depths and concentrations. To this end, a methodology was implemented that would optimize both detection geometry and incident spectrum. Moreover, background subtraction methodologies were carried out, which obtained calibration curves in order to perform quantifications of identified signals.

2. Materials and methods

In order to evaluate the increase in GNP detection capacity, XMI-MSIM Monte Carlo simulations (Schoonjans et al., 2012) were performed using software specifically optimized for the study of X-Ray fluorescence emission. Fig. 1 shows an illustration of the setup.

The configuration modeled was a backscatter detection geometry, with an incident spectrum generated by an X-Ray tube with a tungsten anode operated at a potential difference in the range from 80 to 100 kV and a tube current of 100 mA. The tube output has a beryllium window of 125 μm and copper filters of varying thickness. The source was placed 20 cm away from the 20 cm long side of a cubic phantom, considering tumors of 1–3 cm^3 of volume,

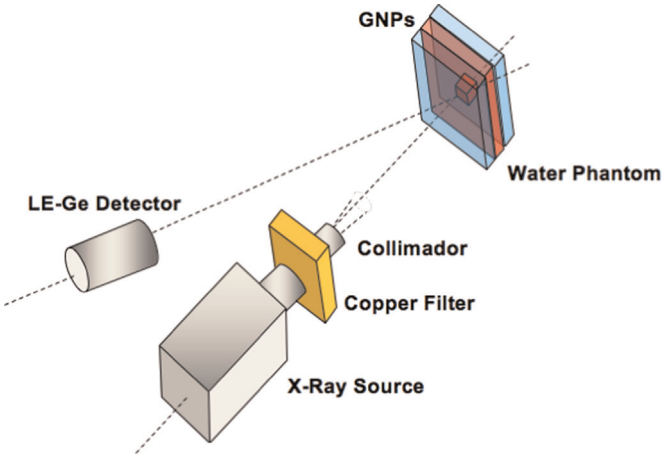

Fig. 1. Geometry of proposed system.

at a depth of 1–5 cm. The phantom was doped with 0.1% to 1% gold particles (range of reported therapeutic values) (Garnica-Garza, 2009) and the simulation-measured time was 10 s. The detector used in the simulation was a solid state LE-Ge of 5 cm of diameter and 2 cm of thickness and a beryllium window.

The maximization of SNR was performed, evaluating the quotient between fluorescence counts versus background for different detection angles, in order to spectrally shift the Compton peak of the area of interest. The dependence of the number of Compton counts according to the angle was taken into account.

In order to evaluate the tuning of the incident spectrum that would generate an optimization of spectral signal identification, detection and uncertainty limits were used as figures of merit. Scanning with energy was begun at the absorption edge. To this end, maximum potential difference applied to the tube was progressively modified. A copper filter of varying thickness was put in the tube in order to remove the lower energy photons from the spectrum. Current intensity was also regulated so as to compare the value of the merit figure according to the energy with the same number of incident photons.

In order to implement a background subtraction methodology, simulation of the tumors without gold nanoparticles was performed, with the express purpose of evaluating only the scattering distribution within spectral areas of interest. This made it possible to subtract only the fluorescence counts from the spectra containing variable concentrations of gold. Finally, calibration curves for different depth (1, 3 and 5 cm) were obtained from the number of fluorescent counts from determined Kb lines following removal of the background, as a function of concentration of gold nanoparticles for therapeutically reported concentration ranges (0.1–1%).

3. Results and discussion

Signal to noise ratio for Kβ lines, in function of the detection angle for an incident energy spectrum centered on the absorption edge, determined that a backscatter geometry of 170° maximizes the above relationship. This produces a great improvement in the ability to identify the fluorescence line in an area of interest with very low background compared to the higher intensity Ka fluorescence line, but in the vicinity of the maximum Compton peak. Fig. 2 shows, in a logarithmic scale, how the shift of the Compton peak dependent on the detection angle defines a geometry in which it is possible to clearly isolate the Kb fluorescence line from the background. These spectra were obtained using a 1 cm^3 tumor at 5 cm depth with a 0.1% concentration of gold nanoparticles.

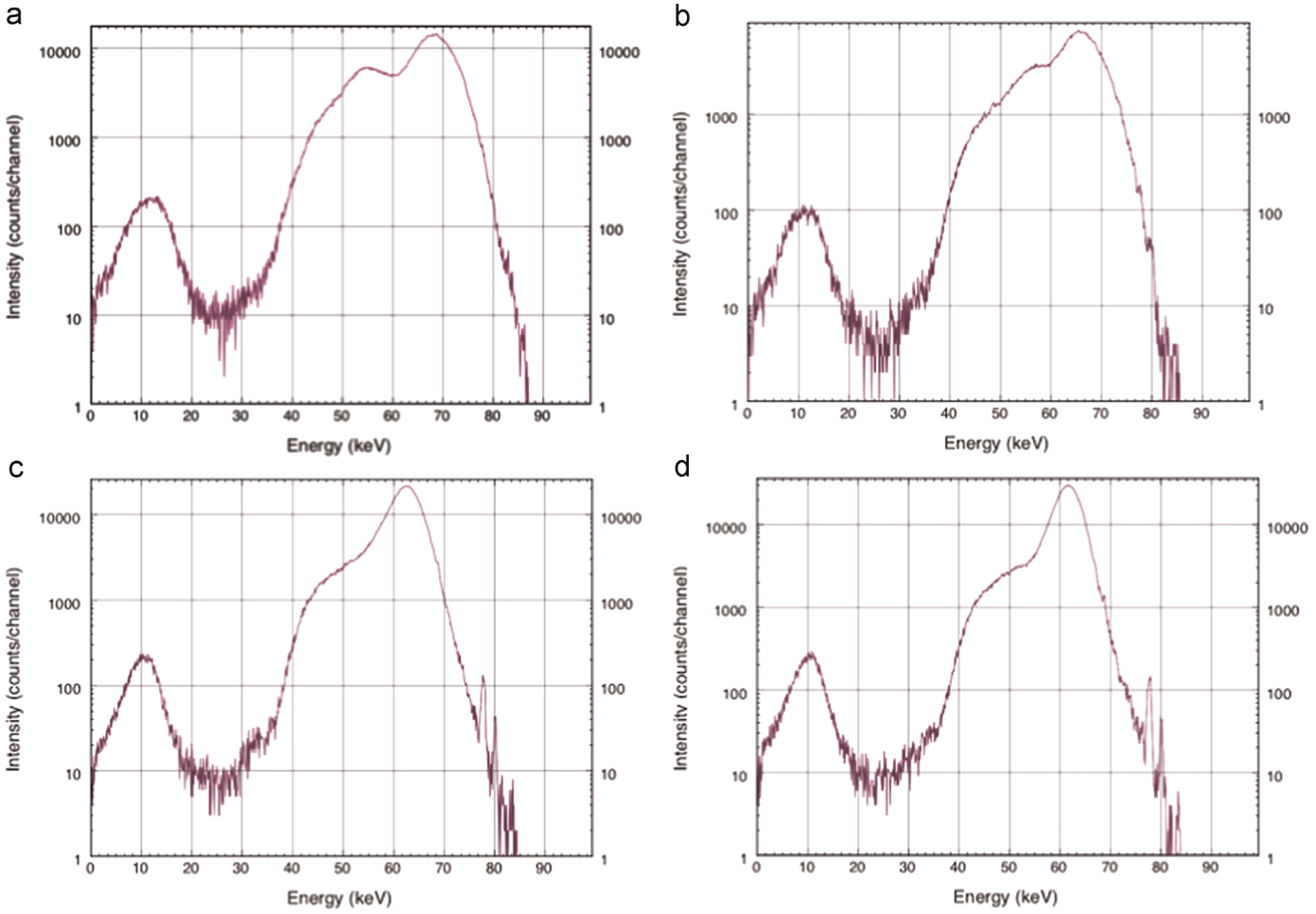

Fig. 2. Improvement in signal to noise ratio for different backscatter geometry: above (a) 90° and (b) 120°, below (c) 150° and (d) 170°.

The evaluation of the incident spectral energy that maximizes the merit figures (which statistically discriminate the improvement of fluorescence line detection) was carried out with a progressive increase of the energy on which the incident spectrum is centered.

The Figs. 3 and 4 show that the detection limit and the uncertainty (in arbitrary unit), associated with the identification of the fluorescence Kβ peak, show a great improvement with a minimum values in the figure of merit, which reaches for incident spectrum energies centered between 83–84 keV. The existence of this minimum is explained as follows: when the energy center of the incident spectrum is shifting from the absorption edge energy to higher values, the increment in the number of fluorescence photon increases more strongly than does the increase in background level produced by the shift of the Compton Peak towards the area of interest. However, for values higher than which specific threshold energy, the shift of the Compton Peak begins an overlap with the studied fluorescence line, thus decreasing accuracy of the spectral identification.

For the range of depths simulated (1–5 cm) is not observed a dependence of the energy value that minimizes the limit of detection and the uncertainty with the depth (see Fig. 3), considering as the parameters of the tubes configuration have a range of error in the tuning peak of 0.3 to 0.4 keV. Greater depths would not be interesting since the application of these techniques mainly restricted to superficial tumors given the limited power of

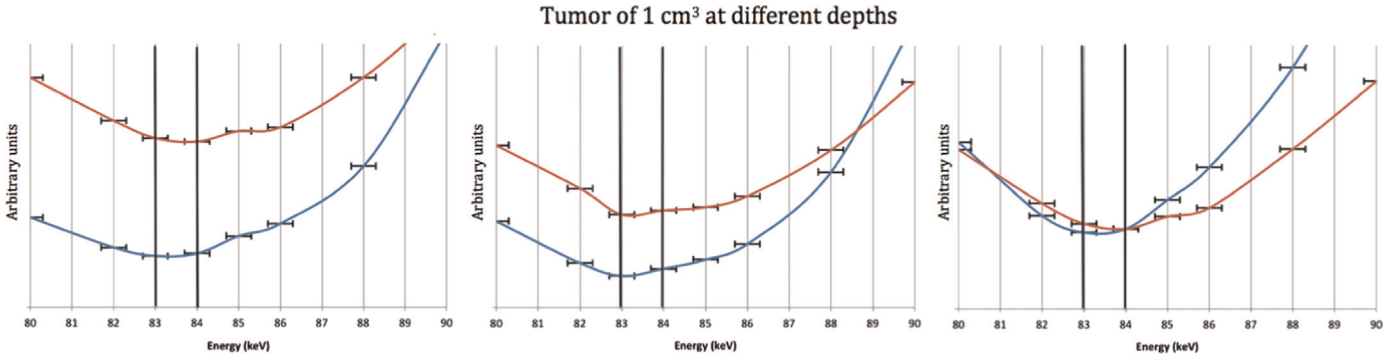

Fig. 3. Detection limit (blue line) and uncertainty (red line) according to incident energy for a tumor of 1 cm^3 at different depths: (a) 1 cm, (b) 3 cm and (c) 5 cm. (For interpretation of the references to color in this figure legend, the reader is referred to the web version of this article.)

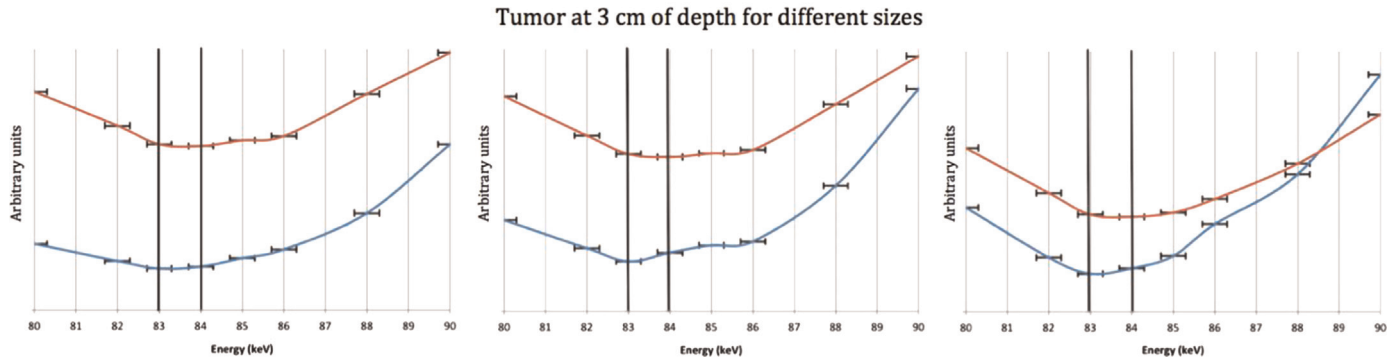

Fig. 4. Detection limit (blue line) and uncertainty (red line) according to incident energy for tumors of different sizes to 3 cm of depth: (a) 1 cm^3, (b) 3 cm^3 and (c) 5 cm^3. (For interpretation of the references to color in this figure legend, the reader is referred to the web version of this article.)

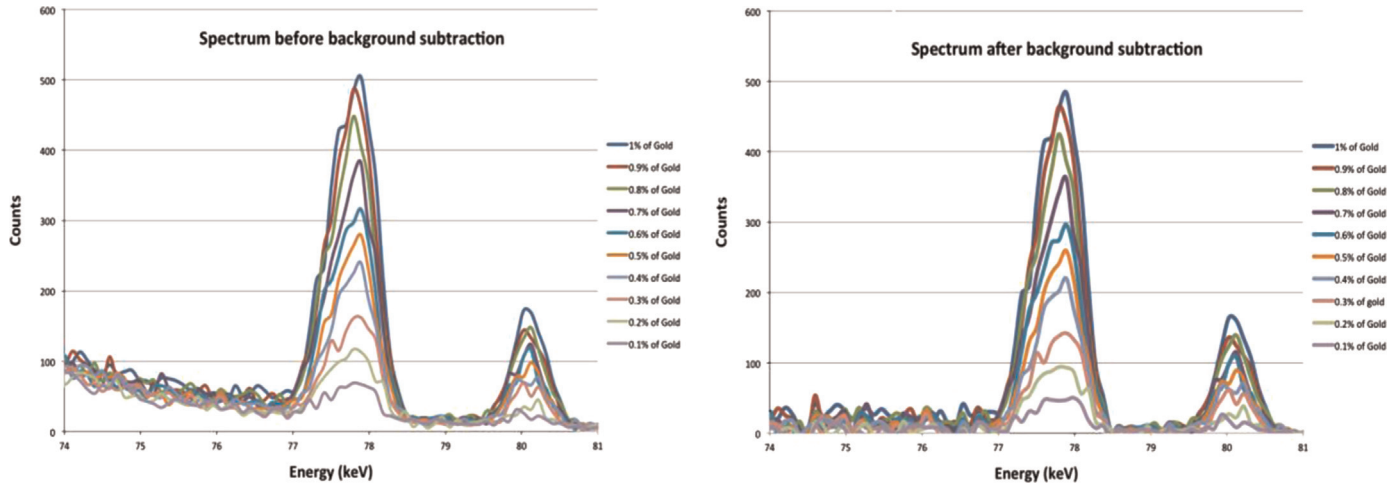

Fig. 5. Spectra of the Kβ line from the simulated tumors of 1 cm^3 to a depth of 3 cm with gold concentrations in a 0.1–1% range before and after applying background subtraction.

penetration of the photons produced in orthovoltage sources. In equal form, for the 3 tumor sizes studied (1, 3 and 5 cm^3) is not observed a dependence of the optimal energy value with the tumor size (see Fig. 4), considering too the error in the tuning peak.

Following the developed methodology, Fig. 5 shows an example of the spectra of the Kβ line obtained for simulated tumors of 1 cm^3 with gold nanoparticle concentrations in a 0.1–1% range before and after applying background subtraction. An adequate detection and energy activation configuration produce a high SNR for the gold Kb line, even before background subtraction. However, the correct discrimination between the fluorescence peak and background signal achieved by the background subtraction methodology makes it possible to decrease uncertainty in analyzed data and obtain more precise calibration curves.

The calibration curves for quantitative analysis, between the number of accounts and GNPs concentration for tumors at different depths were performed (Fig. 6). In these simulations are possible to see that when the tumor is deeper, strongly increases the attenuation in the number of photons that reach from the phantom. The attenuation allow discriminate increased in the concentration only of 0.1% to depths less than 5 cm (considering the sum of the Poisson error of the background and number of total counts). However, is shown which to depths of 5 cm or higher in the range of 0.3–0.8% in concentration it is only possible to discriminate increases with a sensitivity in the range of 0.15–0.2%.

The construction of an appropriate calibration curve requires knowledge of preliminary information on the depth and extent of the tumor, whenever a clinical application is performed. One advantage of the proposal, is given because the experimental setup

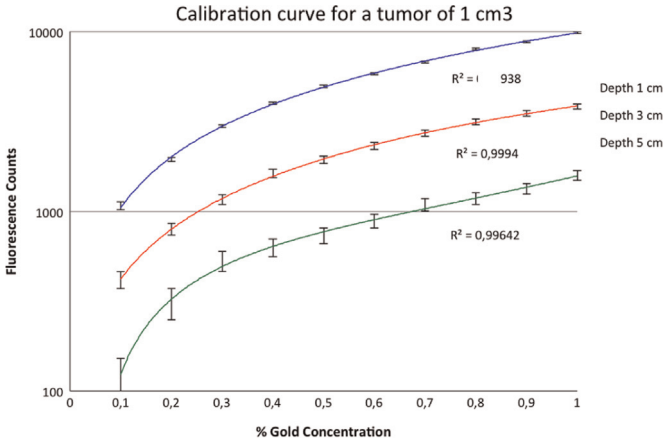

Fig. 6. Calibration curves of the number of counts produced by the Kβ X-ray fluorescence line in function of the gold-nanoparticles concentration for a tumor of 1 cm^3 at different depths. Blue curve 1 cm, red curve 3 cm and green curve 5 cm. (For interpretation of the references to color in this figure legend, the reader is referred to the web version of this article.)

was made considering an traditional X-ray equipment for radiodiagnostic, whereby it is possible to determine a preliminary position of the tumor by conventional radiographic using the properties of the higher contrast level which the GNPs offer (Roeske et al., 2007) and from this information, reconstruct the corresponding calibration curve using the methodology proposed.

An important parameter for assessing the feasibility of the

implementation of X-rays techniques for *in vivo* monitoring is the restriction to the skin entrance dose (dose on the entrance of the phantom in this case) limited to be less than 10 mGy (Wielopolski, 1999). In our setup due to the high attenuation of the filters used in shaping the spectrum, determine a dose to the entrance of the phantom of 1.2 μGy, which would allow future superficial scan applications for evaluate the distribution of GNPs, without reaching the maximum recommended dose. The configured parameters were mainly determined to generate a low dose. Future applications which seeking to implement simultaneous therapy may set an incident spectrum centered in the same predetermined optimum energy but with greater spectral width, to generate a greater delivered dose.

4. Conclusions

Was possible to achieve a better signal to noise ratio in the detection of gold nanoparticles. The results obtained show that a backscatter geometry, a methodology appropriate for the background subtraction and optimum incident energy, allow a strong increase in the SNR in the fluoresce Kβ secondary lines. enabling increased detection sensitivity, lower uncertainty results and lower exposure times. The improve in the number of counts detected for this line allows an improve in the detection limit which will allow used lower amount of gold-nanoparticles and lower price in the implementation.

The results suggest an increase in detected signal that is superior to the values obtained to date, as recorded in the literature (Roeske et al., 2007), and is more similar to clinical conditions. Furthermore, these results were attained for measurement times that allow for superficial scan applications, so as to scan the entire tumor area. This would increase the sensitivity of the technique in future diagnostic and medical imaging applications.

Acknowledgments

This project was supported by MFM-UNC through the project: FM14-003 and the Research Division of the University of La Frontera, DIUFRO, through the project: DI14-6006.

References

Cheong, B., Jones, A., Siddiqi, F., Liu, N., Manohar, M., Cho, S., 2010. X-ray fluorescence computed tomography (XFCT) imaging of gold nanoparticle-loaded objects using 110 kVp X-rays. Phys. Med. Biol. 55, 647–662.

Figueroa, R.G., Lozano, E., Belmar, F., Alcaman, D., Von Bohlen, A., Oliveira, C.A.B., Silva, A.L.M., Veloso, A., 2014. X-Ray Spectrom. 43, 126–130.

Garnica-Garza, H.M., 2009. Contrast-enhanced radiotherapy: feasibility and characteristics of the physical absorbed dose distribution for deep-seated tumors. Phys. Med. Biol. 54, 5411–5425.

Hainfeld, J.F., Slatkin, D.N., Focella, T.M., Smilowitz, H.M., 2006. Size and concentration effect of gold nanoparticles on X-ray attenuation as measured on computed tomography. Br. J. Radiol. 79, 248–253.

Jain, S., Hirst, D.G., O'sullivan, J.M., 2012. Gold nanoparticles as novel agents for cancer therapy. Br. J. Radiol. 85, 101–113.

Moya-Riffo, M., Bennun, L., Sanhueza, V., Santibañez, M., 2013. A procedure for overlapping deconvolution and the determination of its confidence interval for arsenic and lead signals in TXRF spectral analysis. X-Ray Spectrom. 42, 93–99.

Patra, C.R., Bhattacharya, R., Mukhopadhyay, D., Mukherjee, P., 2010. Fabrication of gold nanoparticles for targeted therapy in pancreatic cancer. Adv. Drug Deliv. Rev. 62, 346–361.

Roeske, J.C., Nunez, L., Hoggarth, M., Labay, E., Weichselbaum, R.R., 2007. Characterization of the theorectical radiation dose enhancement from nanoparticles. Cancer Res. Treat. 6, 395–401.

Santibáñez, M., Bennuna, L., Marcó-Parra, L.M., 2013. TXRF quantification of interfering heavy metals using deconvolution, cross-correlation, and external standard calibration. X-Ray Spectrom. 42, 442–449.

Schoonjans, T., Vincze, L., Solé, V., del Rio, M., Brondeel, P., Silversmit, G., Appel, K., Ferrero, C., 2012. A general Monte Carlo simulation of energy dispersive X-ray fluorescence spectrometers, Part 5: polarized radiation, stratified samples, cascade effects, M-lines. Spectrochim. Acta Part B 70, 10–23.

Wielopolski, L., 1999. Design consideration for an EDXRF system for in vivo elemental analysis. Adv. X-Ray Anal. 41, 892–897.

Wu, D., Li, Y., Wong, M.D., Liu, h, 2013. A method of measuring gold nanoparticle concentrations by X-ray fluorescence for biomedical applications. Med. Phys. 40, 051901.